Phase Slips in Oscillatory Hair Bundles

Yuttana Roongthumskul, Roie Shlomovitz, Robijn Bruinsma, and Dolores Bozovic

Phase slips in oscillatory hair bundles

Yuttana Roongthumskul, Roie Shlomovitz, Robijn Bruinsma, Dolores Bozovic

Department of Physics and Astronomy,

CNSI, University of California Los Angeles,

Los Angeles, California 90024, USA

(Dated: February 26, 2013)

Abstract

Hair cells of the inner ear contain an active amplifier that allows them to detect extremely weak signals. As one of the manifestations of an active process, spontaneous oscillations arise in fluid immersed hair bundles of *in vitro* preparations of selected auditory and vestibular organs. We measure the phase-locking dynamics of oscillatory bundles exposed to low-amplitude sinusoidal signals, a transition that can be described by a saddle-node bifurcation on an invariant circle. The transition is characterized by the occurrence of phase slips, at a rate that is dependent on the amplitude and detuning of the applied drive. The resultant staircase structure in the phase of the oscillation can be described by the stochastic Adler equation, which reproduces the statistics of phase slip production.

Hair cells of the inner ear constitute the functional elements that perform mechanical sensing in both the auditory and vestibular systems [1, 2]. They serve as biological transducers that convert mechanical vibrations evoked by incoming sound waves into electrical signals that can be propagated to the brain. These ciliated sensors are immersed in a fluid environment and sustain vibrations against viscous dissipation, utilizing an active amplification process [3]. The auditory system exhibits exquisite sensitivity of mechanical detection: barely audible sounds evoke displacements in the inner ear on the order of angstroms. Estimates of the passive mechanical properties of a hair bundle – comprised of 30-50 stereocilia protruding from the apical surface of the cell body – indicate that its thermal fluctuations in water at room temperature should be almost an order of magnitude higher than the detection threshold. How the auditory system overcomes the effects of noise to achieve its extreme sensitivity is still not fully understood.

Under *in vitro* conditions, hair bundles can exhibit spontaneous oscillations [4]. The oscillations can reach 100 nm in amplitude and were shown to actively expend energy [4, 5]. Significant noise is evident in the spontaneous oscillations, both as higher frequency fluctuations superposed on the oscillations and as variation in the local frequency and phase of the oscillation. Spontaneous oscillations were previously described by equation systems that support a Hopf bifurcation [4–6], with oscillation amplitude vanishing at a critical point. Near this critical point, low-amplitude stimuli produce a frequency-selective high-amplitude response [7]. Prior experiments in the field showed that this innate active motility can be partially phase-locked by signals of far smaller amplitude [4]. In a recent study, we measured the phase-locked amplitude of hair bundle response to stimuli of a broad range of stimulus amplitudes and frequencies and found it to exhibit an Arnold Tongue [8]. At low amplitudes of stimulation, the phase-locked amplitude of spontaneously oscillating bundles suggested that the bundle was phase-locked to the signal by crossing a saddle node bifurcation on an invariant circle (SNIC). In the vicinity of the bifurcation, at frequencies approaching but not coinciding with the natural frequency of the bundle, we observed the occurrence of phase slips in bundle motion, sudden shifts of 2π with respect to the drive.

In this Letter, we show that the phase dynamics of bundle motion follow predictions based on the stochastic Adler equation [9]. We focus on spontaneously oscillating bundles driven by a stimulus that is sufficiently weak so that it has only a negligible effect on the amplitude of innate motility. We observe that the spontaneous oscillations can intermittently phase-lock
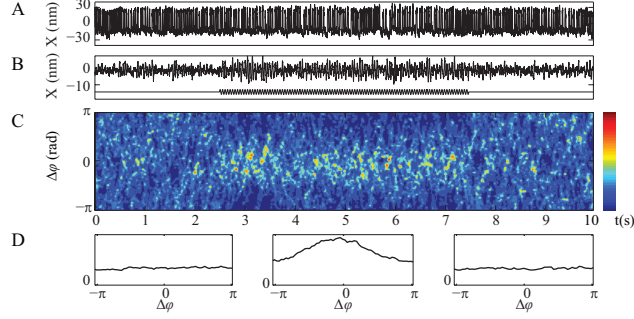
FIG. 1. (Color online) Contraction of the phase distribution induced by a weak stimulus. (A) An example of hair bundle spontaneous oscillations with 1.7 nm stimulus applied from 2.5 to 7.5 seconds. ($\omega = 20$ Hz, $\omega_0 \sim 21.5$ Hz). (B) The averaged response of the bundle (top), performed over 40 presentations, and the stimulus profile (bottom). (C) Time-dependent histogram of $\Delta\phi(t)$. The color-coded scale indicates the height of the histogram in arbitrary units. (D) Time-averaged histogram, in arbitrary units, of $\Delta\phi(t)$ before (left), during (middle), and after the stimulation (right). Histograms of freely oscillating, and driven interval are averaged over 2.5 and 5 seconds, respectively.
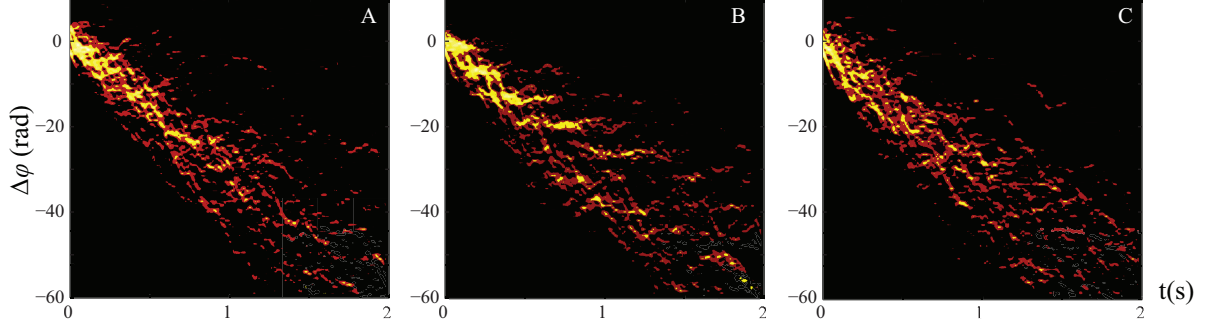

FIG. 2. (Color online) Time evolution of the histogram of the unwrapped $\Delta\phi(t)$ before (A), during (B), and after the stimulation (C). (A), (C) Without stimulus, $\Delta\phi(t)$ is diffusive. (B) During stimulation, plateaus can be observed in the histogram indicating phase-locking in the ensemble response. The color-coded scale indicates the height of the histogram in arbitrary units.

to weak drives, leading to a staircase structure characteristic of a class of nonlinear systems [10]. We demonstrate the presence of phase slips, study the statistics of their occurrence under various drive amplitudes and detuning, and compare the measurements to theoretical predictions.

Experiments were performed on hair bundles of *in vitro* preparations of the bullfrog sac-

3

culus, a vestibular and auditory organ specializing in low-frequency detection. Single hair bundles were imaged with a high-speed CMOS camera and stimulated with glass fibers as described in [11]. At low amplitudes of stimulation (0.2-3 nm), individual traces of hair bundle motion seem unaffected, with the noisy innate oscillation dominating over the sinusoidal signal (Fig. 1A). Upon averaging over multiple presentations, a phase-locked signal emerges (Fig. 1B), indicating that the drive affects the statistics of the phase distribution. In Fig. 1C, we present a 2D plot of the time-dependent probability distribution of the phase difference $\Delta\phi(t) = \phi(t) - \omega t$, with ϕ being the phase of the hair bundle oscillation and ω being the stimulus frequency. The distribution is obtained from 45 presentations of the stimulus. The stimulation amplitude is 1.7 nm, corresponding to the force amplitude (f_0) of ~ 0.4 pN exerted on a perfectly stationary bundle. The stimulus frequency ω is close to the natural frequency ω_0 of the hair bundle. Except when stated otherwise, the instantaneous phase is determined from the phase portrait of displacement and velocity of the oscillations (see Supplement). Note that the statistical distribution of the phase contracts during the stimulus. Time averaged phase distributions for both the free and driven system are shown in Fig. 1D.

The probability distribution of $\Delta\phi(t)$ acquires a more complex structure when the hair bundle is driven by the slightly higher amplitude of 2.5 nm ($f_0 \sim 0.5$ pN) at $\omega > \omega_0$ (15 Hz and 7.5 Hz, respectively). Fig. 2 shows histograms of $\Delta\phi(t)$ obtained from a moving-window fit. During applied stimulus, the phase probability distribution displays plateaus (Fig. 2B), indicating the existence of intervals of phase-locking that are separated by integer multiples of 2π. In Fig. 2A and C, the same analysis was applied to records taken before and after application of the stimulus respectively, with instantaneous phase difference extracted with respect to a zero-amplitude signal. The phase histograms do not exhibit plateaus but rather show a broadening of the distribution that is consistent with phase diffusion (see Supplement).

We next explore phase-locking dynamics in the individual traces. Fig. 3 displays $\Delta\phi(t)$ of one hair bundle as a function of time, extracted from a single trace of motion over the course of the applied stimulus. The sequence of panels corresponds to records taken at increasing f_0. At very small stimuli (Fig. 3A), below ~5 nm (~0.3 pN), the time trace of $\Delta\phi(t)$ drifts linearly with time, consistent with a biased random walk (see Supplement). As the stimulus amplitude is increased (Fig. 3B), plateaus begin to appear in $\Delta\phi(t)$, becoming
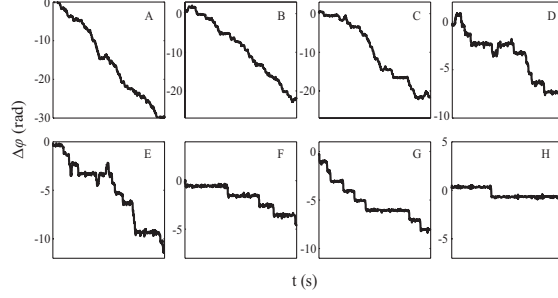
4

FIG. 3. Time evolution of $\Delta\phi(t)$ at different stimulus amplitudes. ($\omega = 10$ Hz, $\omega_0 \sim 14$ Hz). From (A) to (H), f_0 are 0.2, 0.35, 0.5, 0.6, 0.7, 0.8, 1.0, and 1.2 pN, respectively. Phase-locking intervals can be observed for f_0 above ~0.5 pN (C) and extend in duration as the stimulus amplitude increases.

more pronounced with increasing stimulus (Fig. 3C). At drive amplitudes above $\sim$5-10 nm ($\sim$0.3-0.6 pN), the time-dependent traces display intervals of phase-locking, interspersed with phase slips (Fig. 3D-H). Increased levels of stimulus lead to increased durations of the plateaus in $\Delta\phi(t)$, and the reduction in the rate of phase slip production. The direction of the average phase slip is determined by the sign of the detuning ($\omega - \omega_0$).

To extract the characteristics of bundle motion during a phase slip, defined as a change of 2π that occurs on a time scale shorter than the period of the imposed drive, we perform an average over multiple phase slips in individual traces. The detected events are aligned so that the centers of motion coincide (see Supplement). Fig. 4A displays three examples of phase slips, obtained from averages taken over 51, 36, and 31 events, respectively. Fig. 4A *top* and *middle* illustrate the bundle motion during phase slip with positive detuning, where the skip in the oscillation occurs from the positive or negative phase of the active motion. Negative detuning results in an additional oscillation during the phase slip (Fig. 4A *bottom*).

The sensitivity of the hair bundle to the stimulus amplitude indicates that nonlinearity plays a central role in the evoked response. This is consistent with earlier experiments, ranging from *in vivo* measurements of basilar membrane motion in the cochlea to *in vitro* studies of active motility in individual hair bundles of the sacculus, that demonstrated a compressive nonlinearity [4, 7]. In spontaneously oscillating hair bundles exposed to increasing drive amplitude, applied at the characteristic frequency, three regimes of response are observed. At low amplitudes ($\sim$0.1-1 pN), the phase-locked amplitude of the bundle

oscillation ($|\tilde{X}(\omega)|$) increased linearly with the stimulus. Over an intermediate range (1-10 pN), the growth of $|\tilde{X}(\omega)|$ with the imposed drive shows a compressive nonlinearity. Further increase in the stimulus amplitude restores the linear dependence.

To explore the correlation between phase slip production and nonlinearity, we extracted $|\tilde{X}(\omega)|$ from the same hair bundle as shown in Fig. 3, as well as time traces of $\Delta\phi(t)$. In the low stimulus regime, where $|\tilde{X}(\omega)|$ increases linearly with f_0 (blue dots, Fig. 4B), diffusive behavior is observed in $\Delta\phi(t)$ (inset panel b). At f_0 corresponding to the compressive regime (red dots), $\Delta\phi(t)$ exhibits the staircase structure indicative of phase slips (inset panel a). Finally, high drive amplitudes suppress the phase slips and perfectly entrain the motion (inset panel c). In this regime, the amplitude of the phase-locked response is proportional to f_0.

In a prior publication [8], we showed that the main features of the experimentally observed Arnold Tongue could be reproduced by the normal form equation for the Hopf bifurcation. Fig. 4B constitutes a slice through the response space, taken at a fixed frequency. The figure illustrates that the nonlinear growth of $|\tilde{X}(\omega)|$ correlates with the occurrence of phase slips in its $\Delta\phi(t)$. Throughout the regime of weak stimulation (0.1-10 pN), the amplitude of spontaneous oscillation remains constant. Hence, we propose that the relevant variable to describe the dynamics of bundle motion in response to weak signals is the phase degree of freedom. We apply the stochastic form of the Adler equation:

$$\frac{d\Delta\phi(t)}{dt} = -\Delta\omega + \epsilon\sin(\Delta\phi(t)) + \eta(t), \tag{1}$$

where ϵ is proportional to f_0. The detuning term determines the mean phase precession rate. The noise term η satisfies $\langle\eta(t)\eta(t')\rangle = 2T\delta(t - t')$ [12], with T an effective noise temperature. The second term describes the phase locking between the imposed drive and hair bundle motion. The simplest form for this term is that of a sine as it must exhibit a periodic dependence in $\Delta\phi$ with period 2π. Eq. (1) can be obtained from the normal form description of hair bundle dynamics [8] in the limit of weak stimulus. The observed occurrence of phase slips is also captured by more elaborate models of hair cell response, which include adaptation, calcium effects, and other cellular mechanisms [6].

In Fig. 5, we compare our measurements with predictions based on Eq. (1). Fig. 5A displays $|\tilde{X}(\omega)|$, with the analytical prediction $|\tilde{X}(\omega)| = rI_1(\frac{\epsilon}{T})/I_0(\frac{\epsilon}{T})$ at zero detuning superposed [10, 13]. I_0 and I_1 are modified Bessel functions of the first kind, and r is
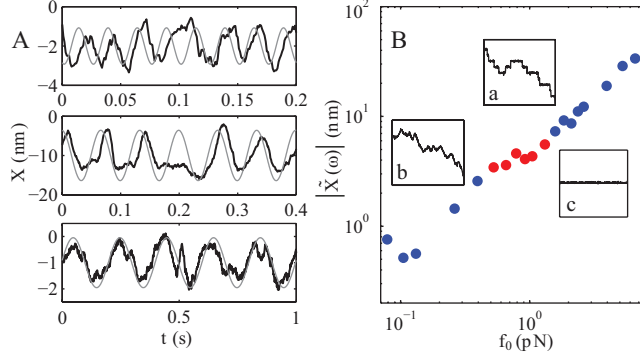
FIG. 4. (Color online) (A) Characteristic dynamics of hair bundle motion during a phase slip. The superimposed gray lines indicate the averaged stimulus during the phase slip. *Top, middle* Phase slip associated with positive detuning ($\omega = 40$ Hz, $\omega_0 = 30$ Hz, and $\omega = 15$ Hz, $\omega_0 = 10$ Hz, respectively). *Bottom* A phase slip associated with negative detuning ($\omega = 5$ Hz, $\omega_0 = 6.5$ Hz). (B) Correlation between the appearance of phase slips and the compressive nonlinearity. Red dots indicate the stimulus amplitudes at which the phase slips occur. Blue dots indicate the linear regimes.

the measured amplitude of spontaneous oscillations. The bundle was stimulated with low $\Delta\omega$ (4.7 rad/s), for 10 seconds. Only the low (diffusive) and intermediate (phase-slipping) regimes are shown. The proportionality constant between ϵ/T_{eff} and f_0 was the only fitting parameter.

Fig. 5B displays the frequency of phase slip production (ν_{ps}), as a function of f_0, from the same recordings as in Fig. 5A. In the limit of small $\Delta\omega$, the rate for thermally activated phase slips is $\nu_{ps} = \frac{\Delta\omega}{2\pi}[I_0(\frac{\epsilon}{T})]^{-2}$ according to Eq. (1) [10, 13]. The relation between ϵ/T_{eff} and f_0 was used as extracted for Fig. 5A. We also examine the dependence of the rate of phase slip production on $\Delta\omega$, at a fixed f_0. The experimental result shows a linear dependence which is consistent with the theoretical prediction (see Supplement).

For stimulus amplitudes that do not induce entrainment, the phase of the bundle oscillation exhibits diffusive behavior. The effective diffusion coefficient (D_{eff}) is determined from the slope of the linear fit to $\langle(\Delta\phi(t+\tau) - \Delta\phi(t))^2\rangle_t$ (see Supplement). D_{eff} obtained from Eq. (1) by numerical integration shows a maximum as a function of the drive amplitude. Fig. 5C compares the measured D_{eff}, from the same hair bundle as Fig. 4A(*Top*), with the theoretical prediction.
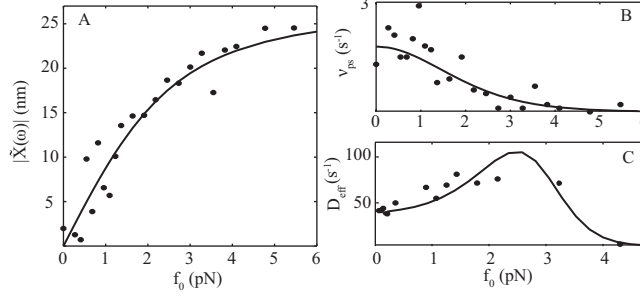
FIG. 5. Comparison with the Adler equation. Analytic solutions (solid line) are superposed on experimental data (dots). (A) Phase-locked amplitude as a function of f_0 ($\omega = 5$ Hz, $\omega_0 \sim 4.5$ Hz). The measured $r = 28$ nm. The proportionality constant $\epsilon/T = 0.66 f_0$, is obtained from the fit. (B) Rate of phase slip production as a function of f_0. The fit of the analytic solution is plotted with the same fitting parameter as in (A), with $\Delta\omega = 4.7$ rad/s. (C) D_{eff} predicted by Eq. (1) and extracted from the data. The proportionality constant $\epsilon/T = 0.63 f_0$ and $D_0 = 40$ s^{-1} are obtained from the fit, with $\Delta\omega$ fixed at the measured value of 60 rad/s.

To further test the validity of the stochastic Adler equation, we also extract ϵ from the averaged Eq. (1), and T from the autocorrelation function of $\Delta\phi(t)$ during phase-locking. The ratio of ϵ/T agrees with the value obtained from the fit (see Supplement).

Prior theoretical studies described the dynamics of the auditory system by proximity to a supercritical Hopf bifurcation [7, 14], shown to capture the amplification and frequency selectivity observed in the cochlea. Here, we examine the response of spontaneously oscillating hair bundles under *in vitro* conditions, indicating that the system is not in the immediate vicinity of a supercritical Hopf bifurcation. We find that the dynamics at low stimulus amplitudes are well described by the stochastic Adler equation, which displays a transition between the spontaneous and mode-locked oscillation. The transition occurs via a SNIC [15] and is characterized by a regime in which the phase difference $\Delta\phi(t)$ between the oscillator and the stimulus displays phase slips. The staircase structure observed in the phase difference is one of the classic signatures of mode-locking in a system described in prior literature by a tilted washboard potential [10].

While the occurrence of spontaneous oscillation under *in vivo* conditions remains unknown, the existence of spontaneous otoacoustic emissions indicates that such an instability can arise. In the presence of spontaneous oscillation, weak signals lead to a contraction

8

in the distribution of instantaneous phase of hair bundles. We observe that, at slightly higher amplitudes of stimulation, contraction in the distribution of phase does not proceed in a uniform fashion, but rather leads to the appearance of phase-locked plateaus in the response. Mode-locked intervals are interrupted by sudden phase slips of 2π, leading to the staircase structure characteristic of this class of nonlinear systems [10]. Hence, even at amplitudes of applied force that are too small to evoke complete entrainment, intermittent intervals of phase locking occur in the active oscillation of individual bundles. We propose that the phase degree of freedom dominates the hair bundle response in this regime, and is well described by the stochastic Adler equation.

Entrainment of active motility by weak signals, with the bundles poised in the regime of intermittent mode-locking, could provide a sensitive mechanism of detection. Crossing of the SNIC bifurcation, however, does not lead to frequency selectivity of the response. The sacculus, a vestibular and auditory organ specializing in low frequencies, is known to have convergent patterns of enervation, with each neuron connected to an ensemble of hair cells. Phase-locking of an ensemble of oscillatory hair bundles constitutes a potential mechanism of detection in biological systems that display high sensitivity and broad frequency tuning.

---

[1] A. J. Hudspeth, Neuron **59**, 530 (2008).

[2] M. A. Vollrath, K. Y. Kwan, and D. P. Corey, Annu. Rev. Neurosci. **30**, 339 (2007).

[3] T. Gold, Proceedings of the Royal Society of London B **135**, 492 (1948).

[4] P. Martin, A. J. Hudspeth, and F. Julicher, Proc. Natl. Acad. Sci. USA **98**, 14386 (2001).

[5] B. Nadrowski, P. Martin, and F. Julicher, Proc. Natl. Acad. Sci. USA **101**, 12195 (2004).

[6] L. Han and A. B. Neiman, Phys. Rev. E **81**, 041913 (2010).

[7] V. M. Eguiluz, M. Ospeck, Y. Choe, A. J. Hudspeth, and M. O. Magnasco, Phys. Rev. Lett. **84**, 5232 (2000).

[8] L. Fredrickson-Hemsing, S. Ji, R. Bruinsma, and D. Bozovic, Phys. Rev. E **86**, 021915 (2012).

[9] A. Pikovsky, M. Rosenblum, and J. Kurths, *Synchronization: A Universal Concept in Nonlinear Sciences* (Cambridge University Press, Cambridge, England, 2001).

[10] M. Tinkham, *Introduction to Superconductivity* (McGraw Hill, New York, NY, 1996).

[11] D. Ramunno-Johnson, C. E. Strimbu, L. Fredrickson, K. Arisaka, and D. Bozovic, Biophys. J. **96**, 1159 (2009).

[12] R. E. Goldstein, M. Polin, and I. Tuval, Phys. Rev. Lett. **103**, 168103 (2009).

[13] V. Ambegaokar and B. I. Halperin, Phys. Rev. Lett. **22**, 1364 (1969).

[14] S. Camalet, T. Duke, F. Julicher, and J. Prost, Proc. Natl. Acad. Sci. USA **97**, 3183 (2000).

[15] S. H. Strogatz, *Nonlinear Dynamics and Chaos* (Westview Press, Cambridge, MA, 1994).